Polar (Acyclic) Isomer of Formic Acid Dimer: Gas-Phase Raman Spectroscopy Study and Thermodynamic Parameters

Roman M. Balabin*

Department of Chemistry and Applied Biosciences, ETH Zurich, 8093 Zurich, Switzerland

Received: January 11, 2009; Revised Manuscript Received: March 3, 2009

The formic (methanoic) acid spectral range of 575−1150 cm^{-1} has been studied by the gas-phase Raman spectroscopy method in a temperature region between 25 and 45 °C. A weak Raman-active vibration of polar (acyclic) HCOOH dimer (a-FAD) has been found at 864 ± 2.1 cm^{-1} and assigned using quantum chemistry data. The contours of the formic acid monomer (FAM) line at 1104 cm^{-1} and the a-FAD line were deconvoluted using *ab initio* data to obtain precise total integral intensities. The temperature dependence of the intensity ratios was used to evaluate the thermodynamic parameters of the polar dimer. Its experimental dimerization enthalpy ($\Delta H_{a\text{-}FAD}$) was found to be −8.6 ± 0.2 kcal mol^{-1}. The entropy of dimerization has been evaluated using theoretical (MP2) Raman scattering activities. Its value ($\Delta S_{a\text{-}FAD}$) is estimated as −36 ± 2 cal mol^{-1} K^{-1}. The results are compared with the published experimental data and calculations. The presented results can be used for molecular dynamics simulations, hydrogen bond energy estimation, and analysis of CH_2O_2 vapor density measurements.

1. Introduction

In recent years, a lot of attention (via both theory and experiment) has been paid to formic acid (HCOOH). The reason for such an interest (compared with an interest in methanol, methane, and even water)[1−6] is that (i) formic acid (FA) is the simplest member of this group of carboxylic acids;[1] (ii) formic acid dimer (FAD) is a prototype of molecular complexes with double hydrogen bond (so it is closely related to the possible building blocks of biomolecules: enzymes, DNA/RNA base pairs, etc.);[2,3] (iii) hydrogen tunneling splitting has been found experimentally in FA C_{2h} dimer;[4,5] (iv) formic acid has environmental importance since FA is present in clouds and fog;[6] (v) FA also plays an important role in human metabolism.[6]

Formic acid is one of the simplest substances having conformational equilibrium[7] (see Figure 1). Its *cis* conformer is less stable (by 3.90 ± 0.09 kcal mol^{-1})[8] and more polar (dipole moment: 3.97 vs 1.42 D).[9]

It should also be noted that tetramers of formic acid are an interesting example of the importance of dispersion interactions even in polar systems.[6,10]

It has been known for many years that molecules of carboxylic acids (formic, acetic, etc.) form dimers in the gas phase, first from the measurement of vapor density,[11,12] followed by spectroscopic observations.[1] Formic acid dimer with C_{2h} symmetry (cyclic FAD or c-FAD; the simplest member of this group) represents the paradigm of symmetric double hydrogen bonding.[13] Its structure has been studied by electron diffraction,[14,15] infrared and Raman spectroscopy (in gas, liquid, and solid phases plus in matrixes and in molecular beams; see ref 13 and the references therein), dielectric spectroscopy, [16−18] NMR spectroscopy,[19,20] laser temperature jump,[21] and shock-tube techniques.[21]

Acyclic formic acid dimer (a-FAD)—an isomer of FA cyclic dimer—is a structure of great importance for formic acid, since low-temperature crystalline acid contains infinite planar chains with neighboring pairs of an a-FAD structure (according to X-ray and neutron diffraction).[22] The large dielectric constant of liquid and solid phases and its temperature behavior confirm the significant contribution of polar structures in liquid and solid formic acid.[18] Also, new experimental and theoretical findings

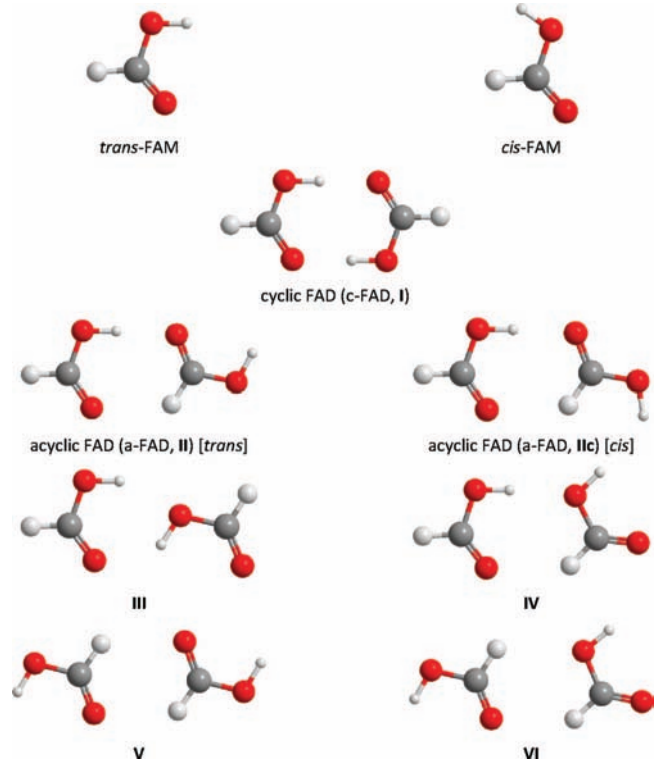

Figure 1. Formic acid monomers and dimers. Monomers, *trans*-FAM and *cis*-FAM conformations; dimers, FAD structures (isomers) **I**−**VI**. The names are given according to ref 23. Dimer structure **IIc** is a conformer of **II** where one formic acid monomer is in *cis* (*E*) conformation.

* Address for correspondence: Tel. +41-44-632-4783; E-mail balabin@org.chem.ethz.ch.

10.1021/jp9002643 CCC: $40.75
Published on Web 04/03/2009

suggest that acyclic dimer is an intermediate structure in a stepwise FA dimerization process.[7]

The MD/Q simulations and *ab initio* studies of Chocholoušová et al.[23] have confirmed that acyclic structure with one O−H···O═C and one C−H···O═C hydrogen bond is a minimum of potential energy surface (PES). Six other isomers of FAD were also identified. A fraction of a-FAD is expected to increase with increasing temperature and pressure.

In studies by Gantenberg et al.,[24] formic acid dimers were investigated by pulse deposition of FA into argon matrices at 7 K. At low temperatures, the results suggested the formation of an acyclic isomer of the dimer.

Madeja et al.[22] have reported the observation of vibrational bands of formic acid dimers, as formed in ultracold helium nanodroplets. For formic acid dimers, the described dimerization process leads to the preferred formation of an acyclic polar dimer. The accompanying theoretical calculations were carried out, which demonstrate that this structure is preferentially formed owing to the fact that the dominating dipole−dipole interaction at long-range geometries favors structures that will lead to the preferred formation of a-FAD when the intermolecular distance is subsequently reduced.[22]

Even though theory predicts and experiment confirms the possibility of acyclic formic acid dimer formation, it still has not been observed at thermodynamically equilibrium conditions. The question of its presence in formic acid vapor is still open. It should also be noted that nowadays no experimental information about binding energy of an acyclic structure is available.

In this paper, we have tried to identify an acyclic (polar) isomer of formic acid dimer (a-FAD) in a gas phase at equilibrium conditions close to the normal ones. The second aim was to try to evaluate its thermodynamic parameters (first of all, enthalpy of dimerization). The method of Raman spectroscopy has been applied. *Ab initio* calculations were used to support our conclusions.

2. Experimental Section

2.1. Raman Setup. A unique 457-nm CW diode-pumped solid state (DPSS) laser, with an output power of 19.8 W and a spectral line width of less than 0.1 nm, was used. The average laser power instability was 5% (for a 12-h period). The laser beam diameter was 1.5 mm.

The laser beam was split into two unequal components with an intensity ratio of approximately 299/1 using a partial reflectance plate beam splitter (beam sampler; 45° geometry). Approximately 0.33% of laser power was sent to a laser power meter equipped with a high-sensitivity thermopile sensor (15-μW power resolution). The result of power measurement was integrated over time with spectra (background) measurement and used for spectra (background) normalization. The remaining 99.67% of the beam power was sent to the gas-phase cell.

A low-temperature retroreflecting multipass cell for Raman spectroscopy was constructed according to ref 25. In brief, a cell was constructed using two planoconvex lenses ($\varnothing = 105$ mm, $f = 400$ mm) with each surface dielectric coated for 99.85% transmission at $\lambda = 457$ nm. The retroreflecting mirrors (75 × 30 mm) were coated for 99.85% reflectivity ($\lambda = 457$ nm) at an angle of 45° and polarization perpendicular to the plane containing the incident and reflected light. The cell was constructed for 67 passes. The gain of the cell was found to be 47.5 ± 0.5 when compared to one-pass variant (according to nitrogen, hydrogen, and *n*-pentane measurements).

The scattered light was collected by a four-lens condenser (Vavilov State Optical Institute, Russia) with a collecting angle of 84° ($\varnothing = 50$ mm). The 90° geometry was used. To intensify the signal, the light scattered over 270° angle (opposite direction) was reflected by a spherical mirror through the scattering center onto the collecting lenses.

The collected light was focused on the entrance slit of a triple spectrometer working in a subtractive mode. Highly effective (2400 g/mm) diffraction gratings were used at all stages. The Raman photons were detected using a back-illuminated 2048 × 512 pixel 16-bit CCD camera of a pixel size of 13.5 × 13.5 μm. The camera was cooled with liquid nitrogen (LN). The quantum efficiency (QE) of the camera was ∼85% in the 400−500 nm region with a maximum at 448 nm. To prevent spectra "contamination" by cosmic rays and natural radioactivity (background radiation), a lead box with 15-cm walls (from the top and three sides) was constructed around the CCD camera.

A Hg lamp was used for wavenumber (*X*-axis) calibration, and pure nitrogen for Raman intensity (*Y*-axis) calibration.

The thermostat enabled attaining the cell temperature with an accuracy of ± 0.01 °C (standard deviation at 50 °C for a 4-h period). A light gas flow (approximately 1 m/s) was organized inside the cell.

The whole setup was placed in a dust-free environmental control chamber with a temperature of 12.0 ± 0.2 °C and a relative humidity of 7 ± 2% (to stabilize it). The setup was extremely sensitive to dust and contamination of optical elements.

2.2. Experimental Parameters. The temperature range from 25 to 45 °C (298−318 K) was scanned with a step of 1.00 ± 0.04 °C. The same range in "$10^5/T$"-scale is 398−368 K^{-1} with a step of 1.054 K^{-1} (21 points). A constant formic acid vapor pressure of 4500 Pa (∼34 torr) was used.

The slit width of the spectrometer was set to 100 μm (unless otherwise specified in the text). It corresponds to ∼2 cm^{-1} of spectral resolution. Only the stokes part of FA spectrum has been analyzed.

The duration for collecting one spectrum was 5 min. During this period, 15 sample spectra and 15 background spectra were collected one-by-one (10 s of accumulation time each). Because of the great difference in signal intensities to collect enough signal of acyclic dimer, overflowing of CCD chip at other frequencies was needed. Three more spectra (1, 3, and 6 s) were collected, and extrapolation to the 5 min value has been done.

The system has been left for 5 min for thermostatting before each measurement.

Seven spectra were collected at each temperature with a 2-day time interval. Five best values (all inside $\pm 3\sigma$ interval) were used for averaging.

Extra steel sheets have been put at the bottom of the cell to vary the surface-to-volume (S/V) ratio for adsorption correction. The S/V values from 0.25 (no sheets) up to 1.41 cm^{-1} (12 sheets) have been achieved. The glass-to-steel surface ratio has been kept constant in all the experiments. See section 3.2.1 for details.

2.3. Materials. Formic acid (≥85%, reagent grade) was obtained from Chimmed (Moscow, Russia). It was dried for 30 h over anhydrous copper(II) sulfate and then vacuum distilled (five times) at room temperature. The distilled product was purified by the fractional crystallization (fractional freezing). This method was applied up to 14 times to reach product purity better than 99.95%. The purity was checked by gas chromatography (GC) and titration with standard base using a weight buret. Vapor pressure measurements have confirmed acid purity.

The fresh substance was stored frozen (−150 °C) in argon atmosphere for not more than 5 days to prevent its decomposition.

TABLE 1: Formic Acid *Trans* Monomer Geometry: Experimental and Predicted[a]

	exp[b]	CCSD(T)/aug-cc-pVTZ[c]	MP2/6-311++G(3df,2p)	B3LYP/6-311++G(3df,2p)
r_{C-H}	109.7 ± 2.1	108.9	109.3	109.7
$r_{C=O}$	120.2 ± 0.3	119.9	120.2	119.6
r_{C-O}	134.3 ± 0.3	134.3	134.4	134.4
r_{O-H}	97.2 ± 1.7	96.7	96.9	97.0
$\alpha_{H-C=O}$	124.1 ± 3.1	125.1	125.2	125.2
$\alpha_{O=C-O}$	124.6 ± 0.5	125.1	125.0	125.1
α_{C-O-H}	106.3 ± 0.4	106.3	106.6	107.8

[a] Units: distances (r) are in pm, angles (α) are in deg. [b] Experimental, refs 28, 54, and 57. [c] Unfrozen core, ref 27.

Physical properties: $\rho_{25} = 1213.9 \pm 0.1$ kg m^{-3} (lit, 1214.05 kg m^{-3}),[26] $n^{25}{}_D = 1.3694 \pm 0.000\,15$ (lit, 1.369 38).[26]

It should be noted that not proper formic acid purification leads to a weak Raman peak at 906(1) cm^{-1} appearance. It could be attributed to methyl formate (?).

2.4. Formic Acid Monomers and Dimers Nomenclature. Formic acid monomer (FAM) has two possible conformations (Figure 1): *trans* (*Z*) with a 180° HCOH angle and *cis* (*E*) with a 0° angle. *trans*-FAM (energy minimum[27]) is used as a default monomer structure in the following text (so, FAM = *trans*-FAM). An alternative notation is sometimes used in the literature.[28,29] The *cis* conformer of HCOOH is higher in energy[8] by 3.90 ± 0.09 kcal mol^{-1} (experimental value). Császár et al.[27] reports the value of 4.21 kcal mol^{-1} (based on high-level *ab initio* analysis).

Unfortunately, nowadays no universally recognized nomenclature of formic acid dimers (FADs) exists. Each author presents his (or her) own names for different dimer structures (see refs 23 and 29 as examples). In this paper, we will use the FADs names of Chocholoušová et al.[23] Figure 1 presents the structures and their names (**I**−**VI**).

The use of number for dimer designation is not the best choice, as this symbol does not contain any information about dimer structure. The name "cyclic-FAD" or c-FAD is widely used as a name of **I**[7] (the structure with C_{2h} symmetry). Even though this name is informative, it is not unambiguous: the same name is appropriate for structure **V** (C_{2h}).

The name "polar"[23] (in contrast to **I** with a zero dipole moment) or "acyclic"[7] is used for structure **II**. Unfortunately, by using it, it is not possible to distinguish structures **II**−**IV** and **VI**, since all of them have a nonzero dipole moment.

Alternative universal nomenclature should include the designation of H-bond types to be informative and unambiguous. Attempts have been made in refs 22, 29, and 30. Table 5 represents the possible nomenclature of this kind.

One should note that conformation equilibrium is possible not only in formic acid monomer but also in dimers.[29] The structure of such a dimer (**IIc** = *cis*-**II**) is presented in Figure 1 as an example. A similar structure is possible for dimers **III**, **V** (*trans*−*trans*, *cis*−*trans*, and *cis*−*cis*), and **VI**. Even though such conformers are energetically unfavorable, they can appear in formic acid at higher temperatures.

2.5. Quantum Chemistry Calculations. Structure optimization (quadratic approximation algorithm) of formic acid monomer (FAM) and dimers (FADs) was done using PC GAMESS[31] software. C_s (**II**−**IV**, **VI**) and C_{2h} (**I**, **V**) symmetry has been applied. Tight optimization criterion (maximum gradient, 2.5 × 10^{-5}; root-mean-square gradient, 8.3 × 10^{-6} hartree bohr^{-1}) was applied for all structures. Eigenvalues of the Hessian matrix were used to check whether the presented geometry is a potential energy surface (PES) minimum point (not a saddle point).

The second-order Møller−Plesset (MP2)[32,33] level of theory and B3LYP[34] hybrid density functional theory (DFT) method were applied for geometry optimization and harmonic frequencies calculation. A 6-311++G(3df,2p) Pople-type basis set (implemented in PC GAMESS program) was used.

Basis set superposition error (BSSE) correction has been done by standard counterpoise (CP) scheme (after geometry optimization).

Theoretical Raman intensities and depolarization ratios have been obtained by applying an electric field of 2·10^{-3} au (1.028·10^9 V/m).

The enthalpy/entropy difference is reported relative to the double energy of *trans*-formic acid monomer.

2.6. Spectra Deconvolution. It is a well-known fact that a correct mathematical treatment of spectroscopy data can greatly improve the results.[35−42] Spectra deconvolution[43] into rotational branches, similar to that in refs 44−46, was applied. The main difference was the presence of five rotational branches in the case of the Raman spectrum (O-, P-, Q-, R-, and S-branch).[47] MP2/6-311++G(3df,2p) and B3LYP/6-311++G(3df,2p) structure parameters were used. Extra parameters (relative intensities, etc.) were adjusted by robust least-squares procedure[44] until the minimal difference with experimental spectra was achieved. No correction for centrifugal distortion was introduced.

2.7. Software and Computing Inaccuracy. The MATLAB computing environment was used for data analysis. Spectra deconvolution using Gaussian-type instrument function was applied (not to be confused with rotational structure deconvolution). One hundred and five (105 = 21 × 5) data points were used for fitting.

A self-written program for deleting hotlike pixels, produced by cosmic rays and natural radioactivity (background radiation), was used (see ref 48 for details).

Unless otherwise specified, a 95% confidence interval is reported as the measure of inaccuracy.

3. Results and Discussion

3.1. Calculations: Geometries, Frequencies, and Interaction Energies of Formic Acid Monomer and Dimers. ***3.1.1. Geometry of Formic Acid Monomer and Dimers.*** Table 1 summarizes the *ab initio* results for formic acid *trans* monomer structure prediction. The mean absolute difference in interatomic distances (bond lengths) is 0.41, 0.19, and 0.22 pm for CCSD(T)/aug-cc-pVTZ, MP2/6-311++G(3df,2p), and B3LYP/6-2311++G(3df,2p), respectively. The mean absolute difference in angles is 0.41°, 0.53°, and 0.92°, respectively.

It is well seen from Table 1 that even though the CCSD(T) level with greater basis set should produce better results, it is not observed. The reason could be that an error compensation occurs when the MP2 level is applied or experimental data of greater accuracy are needed to evaluate the CCSD(T) level efficiency. It should be noted that only B3LYP/6-311++G(3df,2p) predictions for $r_{C=O}$ and α_{C-O-H} are outside the experimental confidence interval.

TABLE 2: Geometry of Cyclic Formic Acid Dimer (c-FAD, I): Experimental and Predicted[a]

		MP2		B3LYP	
	exp[b]	aug-cc-pVTZ[b]	6-311++G(3df,2p)	aug-cc-pVTZ[b]	6-311++G(3df,2p)
r_{C-H}	107.9 ± 2.1	109.6	109.2	109.5	109.6
$r_{C=O}$	121.7 ± 0.3	122.4	122.0	121.8	121.7
r_{C-O}	132.0 ± 0.3	131.3	131.2	131.0	130.9
r_{O-H}	103.3 ± 1.7	100.0	99.5	100.2	100.1
$r_{O\cdots H}$	−	165.4	169.2	166.7	167.5
$r_{O\cdots O}$	270.3[d]	−	268.7	−	267.6
$\alpha_{H-C=O}$	115.4 ± 3.1	121.9	122.1	121.8	121.9
$\alpha_{O=C-O}$	126.2 ± 0.5	126.3	126.2	126.3	126.3
α_{C-O-H}	108.5 ± 0.4	109.5	109.5	110.9	110.8
$\alpha_{O\cdots H-O}$	180[e]	180.0	179.4	178.5	178.4
A	6064 ± 1[c]	−	6059	−	6064
B	2302 ± 3[c]	−	2271	−	2289
C	1665 ± 3[c]	−	1651	−	1662

[a] Units: distances (*r*) are in pm, angles (α) are in deg, rotational constants (*A*−*C*) are in MHz. [b] References 28, 54, and 57. [c] Reference 30. [d] Reference 58. [e] Assumed in refinement of electron diffraction data.

TABLE 3: Formic Acid *Trans* Monomer Frequencies (cm^{-1}): Experimental and Predicted

				MP2		B3LYP	
	vibration		exp[b]	aug-cc-pVTZ	6-311++G(3df,2p)	aug-cc-pVTZ	6-311++G(3df,2p)
ν_1	O−H	A′	3569	3740	3742	3717	3710
ν_2	C−H	A′	2943	3094	3140	3051	3059
ν_3	C=O	A′	1777	1793	1801	1811	1814
ν_4	H−C=O	A′	1381	1400	1412	1401	1403
ν_5	H−O−C	A′	1223	1301	1304	1298	1297
ν_6	C−O	A′	1105	1130	1133	1122	1122
ν_8	H−C−O[a]	A″	1033	1056	1056	1051	1050
ν_9	H−O−C[a]	A″	642	680	679	678	680
ν_7	O−C=O	A′	625	626	625	629	627

[a] Out-of-plane (o.o.p.). [b] References 28, 54, and 57.

The MP2 and B3LYP prediction of formic acid dimer **I** (cyclic FAD) geometry is shown in Table 2. One can conclude that the use of the 6-311++G(3df,2p) basis set (274 basis functions) instead of aug-cc-pVTZ (368 basis functions) does not worsen the geometrical results (especially at the DFT level). Since geometry optimization with Pople-type basis set is roughly three times less time-consuming, it can be recommended.

It should be noted that the B3LYP/6-311++G(3df,2p) prediction of FAD **I** rotational constants is almost perfect: the average absolute difference is just 5.7 MHz, or 0.17%.

3.1.2. Frequencies of Formic Acid Monomer and Dimers. Vibrational analysis of *trans*-HCOOH is presented in Table 3. Experimental and predicted (harmonic) frequencies are in good agreement. B3LYP and MP2 levels produce results of approximately the same quality: the average relative difference between experimental and *ab initio* frequencies is 3.2%, 3.6%, 3.0%, and 3.0% for MP2/aug-cc-pVTZ, MP2/6-311++G(3d,2p), B3LYP/aug-cc-pVTZ, and B3LYP/6-311++G(3d,2p) levels, respectively. The main discrepancy (46 cm^{-1}) is found for the ν_2 (C−H) vibration at the MP2 level with different basis sets. It could be due to the difference of hydrogen description by aug-cc-pVTZ (two d-functions) and 6-311++G(3df,2p) basis sets. The same difference at the B3LYP level is just 8 cm^{-1}.

Table 4 summarizes the results of FAD **I** vibrational analysis. The situation with dimer is close to that with monomer: the average relative difference between experimental and *ab initio* frequencies is 5.4%, 4.8%, 5.5%, and 5.2% for MP2/aug-cc-pVTZ, MP2/6-311++G(3d,2p), B3LYP/aug-cc-pVTZ, and B3LYP/6-311++G(3d,2p) levels, respectively. It should also be noted that in the case of FAD, ambiguousness with low-frequency vibrations (ν_7, ν_8, ν_9, and ν_{12}) exists.

Frequencies and interaction energies of all formic acid dimers discussed here (**I**−**VI**) are presented in Table 5. The results are in good agreement with the results of Chocholoušová et al.[23,49] FAD **II** is predicted to be ∼5.6 kcal mol^{-1} above structure **I**, so one can expect to find it in a gas phase even at room temperature. Experimental identification of other FADs is expected to be of great difficulty. Energy analysis also shows that *cis* conformer of FAD **II** (**IIc**) has approximately the same energy as structure **IV** and is more stable than dimers **V** and **VI**.

One should also note that comparison of FAD **I** and **II** (**V**) is a comparison of O−H···O=C and C−H···O=C type hydrogen bonds.

Quantum chemistry at the MP2/6-311++G(3df,2p) level predicts that different FAD isomers can be distinguished, especially in a spectral region below 1000 cm^{-1}. But even the difference in C−H and O−H regions (that are extremely complicated)[28] has allowed Madeja et al.[22] to distinguish them. The difference between MP2/6-311++G(3df,2p) and MP2/aug-cc-pVDZ (unscaled) was found to be 2.3% and 1.2% for C−H and O−H regions, respectively.

One can conclude that investigation of formic acid monomer and dimers at MP2/6-311++G(3df,2p) or B3LYP/6-311++G(3df,2p) levels of theory provides results (geometry, energy, and vibrations) that are close enough to experimental values. It seems to be that vibrations' anharmonicity is a more important factor than electron correlation influence (at the MP2/6-311++G(3df,2p) level and higher).

3.2. Raman Spectroscopy: Correction for Formic Acid Decomposition and Adsorption. ***3.2.1. Correction for Formic Acid Decomposition.*** It is a well-known fact that even at room temperature formic acid slowly decomposes into water and

TABLE 4: Experimental and Predicted Frequencies (cm^{-1}) of Cyclic Formic Acid Dimer (c-FAD, I)[a]

				MP2		B3LYP	
	vibration		exp[c]	aug-cc-pVTZ	6-311++G(3df,2p)	aug-cc-pVTZ	6-311++G(3df,2p)
ν_{17}	O−H	B_u	3110	3305	3285	3161	3222
ν_2	C−H	A_g	2949	3137	3182	3066	3113
ν_{18}	C−H	B_u	2957	3132	3152	3055	3036
ν_1	O−H	A_g	−	3194	3148	3040	3030
ν_{19}	C═O	B_u	1754	1776	1778	1767	1770
ν_3	C═O	A_g	1670	1711	1716	1693	1699
ν_4	H−O−C	A_g	1415	1499	1478	1481	1481
ν_{20}	H−O−C	B_u	− (1450[d])	1473	1454	1449	1449
ν_5	H−C═O	A_g	1375	1429	1412	1404	1406
ν_{21}	H−C═O	B_u	1362	1422	1406	1402	1402
ν_{22}	C−O	B_u	1218	1257	1263	1260	1261
ν_6	C−O	A_g	1214	1249	1258	1257	1256
ν_{13}	H−C−O[b]	A_u	1060	1114	1111	1102	1101
ν_{10}	H−C−O[b]	B_g	1050	1085	1084	1079	1077
ν_{14}	H−O−C[b]	A_u	917	995	1002	1002	1008
ν_{11}	H−O−C[b]	B_g	− (920[g]; 922[h])	980	981	983	987
ν_{23}	*O−C═O*	B_u	699	719	712	723	725
ν_7	O−C═O	A_g	677 (680[f])	688	682	690	692
ν_{24}	D i.p. rock	B_u	248	280	272	281	271
ν_{12}	D o..op. wag	B_g	230 (242[f])	269	258	262	260
ν_8	D i.p. rock	A_g	190 (194[f])	209	205	213	206
ν_{15}	D o.o.p. wag	A_u	163	183	184	187	186
ν_9	D stretch	A_g	137 (165[f])	171	164	175	177
ν_{16}	D twist	A_u[e]	68	69	68	78	76

[a] Symmetry is assigned according to refs 7 and 57. D = dimer; o.o.p. = out-of-plane; i.p. = in-plane. Mean absolute deviation (MAD): 58.9, 57.7, 41.7, and 45.8 cm^{-1} for MP2/aug-cc-pVTZ, MP2/6-311++G(3df,2p), B3LYP/aug-cc-pVTZ, and B3LYP/6-311++G(3df,2p), respectively. [b] Out-of-plane (o.o.p.). [c] Reference 57. [d] Reference 7 [e] B_u symmetry is assigned in the Supporting Information of ref 7. [f] Reference 13 (jet-cooled Raman data). [g] Reference 53. [h] This work.

carbon monoxide[12] (or hydrogen and carbon dioxide[50]). Even though the decomposition reaction rate is very small, we cannot neglect it, since we are in need of highly precise data (band intensities).

For such a decomposition correction, a long "background" experiment has been conducted. The formic acid vapor (at a pressure of 4500 Pa) has been left in a setup cell for 30 h under constant temperature of 45 °C (the highest in our series of experiments). The Raman signals of CO and CO_2 have been measured every 1 and 2 h, respectively.

The decomposition reaction rate constant has been evaluated using linear regression of the CO-signal time dependence. The rate constant was found to be $(2 \pm 1) \times 10^{-4}$ h^{-1}. This means that less than 0.005% of the substance decomposes during a 10-min period under the presented experimental conditions. This figure is too small to influence our measurements.

3.2.2. Correction for Formic Acid Adsorption. Carboxylic acids have a well-known tendency to be adsorbed by different surfaces. The importance of this factor on spectroscopic investigations has already been shown.[12,51] The adsorbed CO_2H_2 mass value of ~1 mg per 1 m^2 of glass surface has been reported.[12]

Unfortunately, correction for formic acid adsorption on experimental setup components is not widely used, even though a great influence of this factor on experimental thermodynamic values has been shown.[51] It is obvious that if acid molecules are indeed adsorbed on the surface (glass or metal), van't Hoff isochore is no longer a valid indication of dimerization enthalpy.

A simple but effective procedure for adsorption correction has been suggested by Mathews and Sheets.[51] They have varied the surface-to-volume ratio (S/V) in their experimental setup and have extrapolated the enthalpy difference values to zero surface (S/V = 0).

A similar procedure has been applied in our case, but the Raman signal (not enthalpy) has been extrapolated. This method is expected to produce more reliable enthalpy values, since a linear relationship between adsorbed substance amount and number of Raman photons is expected. The plots in Figure 2 confirm the fact that the Raman signal linearly decreases with increase in surface area. It is observed that the difference in Raman intensities (no extra surface, S/V = 0.25 cm^{-1}), observed at different temperatures, may be just due to the different amounts of absorbed acid. If accuracy better than ~1% is needed, the adsorption correction is necessary. At lower temperatures and higher total pressures, adsorption influence becomes greater.

3.3. Spectrum Analysis. Thermodynamics: Enthalpy and Entropy Difference of Polar (Acyclic) FAD. ***3.3.1. Raman Spectrum Analysis.*** An experimental Raman spectrum example (25 °C; 575−1150 cm^{-1}) is presented in Figure 3. The frequency range between 600 and 1100 cm^{-1} contains information about main formic acid structures occurring at room temperature and at a pressure of 4.5 kPa.

The shape of the lines is rather standard for Raman vibrations: one intense Q-branch and four wide O-, P-, R-, and S-branches. The whole peak area should be integrated to get a precise intensity value.[52]

The peaks at 626.2(2), 1033.5(6), and 1104.2(2) cm^{-1} belong to formic acid monomer (FAM) (see Table 3); the peaks at

TABLE 5: Predicted Frequencies, Raman Cross Sections, and Interaction Energies of Formic Acid Dimers (FADs I−VI) at the MP2/6-311++G(3df,2p)] Level of Theory

	I (c-FAD)	**II** (a-FAD)	**IIc**	**III**	**IV**	**V**	**VI**
alternative notation	O−H···O=C/ O−H···O=C	O−H···O=C/ C−H···O=C		O−H···O−C/ O−H···O=C	O−H···O−C/ C−H···O=C	C−H···O=C/ C−H···O=C	C−H···O−C/ C−H···O−C
symmetry	C_{2h}	C_s	C_s	C_s	C_s	C_{2h}	C_s
ΔE,[a] kcal/mol	−14.46[b]	−8.82	−5.44	−6.80	−5.60	−3.87	−2.93
ΔS,[c] cal mol^{-1} K^{-1}	−43.7	−37.5	−37.8	−34.1	−34.0	−31.2	−27.2
	frequencies (Raman cross section) [MP2/6-311++G(3df,2p)]						
number	value, cm^{-1} (10^{-36} m^2 sr^{-1})						
1	68 (0)	60 (0)	61	16	32	35	29
2	164 (32)	101 (98)	108	70	83	69	55
3	184 (0)	111 (4)	119	129	94	73	55
4	205 (8)	144 (13)	149	144	123	84	59
5	258 (135)	191 (7)	191	180	154	86	81
6	272 (0)	202 (126)	205	225	155	95	91
7	682 (50)	645 (34)	567	653	624	633	625
8	712 (0)	681 (25)	675	679	645	637	632
9	981 (2)	699 (4)	683	750	666	685	674
10	1002 (0)	930 (1)	940	846	823	687	686
11	1084 (11)	1074 (6)	1076	1055	1065	1077	1069
12	1111 (0)	1094 (2)	1078	1070	1068	1079	1073
13	1258 (44)	1161 (17)	1156	1144	1094	1131	1117
14	1263 (0)	1216 (22)	1223	1191	1193	1147	1140
15	1406 (0)	1322 (16)	1295	1304	1273	1313	1291
16	1412 (32)	1385 (13)	1389	1362	1370	1316	1315
17	1454 (0)	1412 (18)	1427	1409	1410	1404	1412
18	1478 (26)	1443 (18)	1444	1434	1433	1408	1414
19	1716 (118)	1749 (107)	1765	1773	1784	1777	1787
20	1778 (0)	1785 (5)	1808	1807	1804	1794	1794
21	3148 (0)	3089 (170)	3115	3117	3097	3161	3135
22	3152 (443)	3153 (69)	3128	3126	3161	3162	3148
23	3182 (139)	3471 (145)	3378	3535	3648	3749	3773
24	3285 (0)	3787 (55)	3866	3691	3767	3749	3788

[a] MP2/6-311++G(3df,2p); BSSE corrected; no ZPE correction. [b] Compare with $\Delta H_{T=0K}$ value of −14.72 kcal/mol.[59] [c] Evaluated at 298.15 K and 4.5 kPa using *ab initio* frequencies in RRHO approximation.

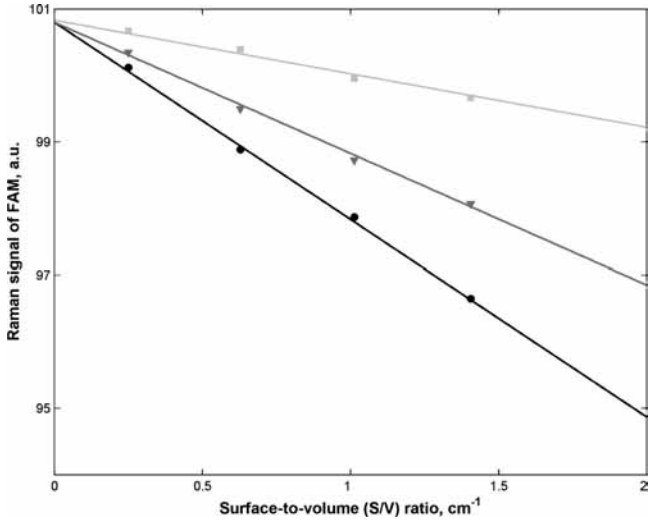

Figure 2. Dependence of formic acid monomer (FAM) Raman signal (at 1104 cm^{-1}) on surface-to-volume (S/V) ratio. Three sets of data points (at three different temperatures) are shown together with their linear approximations: 25 °C (black circles), 35 °C (dark gray triangles), and 45 °C (light gray squares). The Raman intensities are extrapolated to "zero surface" (S/V = 0) before use.

679.8(6), 922.0(15) [ν_{11}], and 1050.0(3) cm^{-1} belong to FAD **I** (see Table 4). It should be noted that the Raman cross section of the ν_{11} vibration is so small (an order of magnitude lower than that of ν_{10}) that it has not been observed in the spectrum of Bertie and Michaelian.[28] Kirklin[53] place it at 920 cm^{-1}. These facts and our procedure of Raman peak deconvolution partly explain the difference in 0.5−3.5 cm^{-1} between our data and the earlier obtained data.

The monomer and dimer vibrations at 1033 and 1050 cm^{-1} were observed as one broad peak in ref 28. The resolution of 11 cm^{-1} has not allowed the authors to distinguish these peaks (see Figure 3 in ref 28). This paper also describes a $\nu_7 + \nu_{12}$ (B_g) vibration at 889 ± 6 cm^{-1} (90%) that we have not found.

A very small peak at 864.1(21) cm^{-1} is expected to be a FAD **II** ν_{14} vibration that is predicted to be at 930 cm^{-1}. Even though the difference between observed and predicted values is rather high (7.1%), the peak's position cannot be called unexpected, since the same situation is found for c-FAD (**I**) ν_{11} and ν_{14} frequencies: the difference in this case is 6.1% and 7.8%, respectively (see Table 4; c-FAD ν_{14} vibration is not Raman active). It can be concluded that out-of-plane H−O−C vibrations of formic acid dimers are highly anharmonic (see Conclusions).

Note that *cis*-HCOOH cannot be regarded as a candidate for the 864 cm^{-1} peak, as its first three low-lying vibrations are at 531, 654, and 1033 cm^{-1} (according to MP2 calculation). All of them are low Raman active (~7 × 10^{-36} m^2 sr^{-1}).

Depolarization ratio of the 864 cm^{-1} peak is 0.743(11). It confirms our assignment since the theoretical value is 0.75.

Using data from Table 5, it is obvious that the vibration at 864 cm^{-1} is the only truly unique frequency for **II**. All other (corrected) frequencies are "masked" by monomer or FAD **I** peaks (except that at 60 and 3471 cm^{-1}). The region below 150 cm^{-1} is full of FAM pure rotational transitions,[13,28] and the C−H/O−H region is too complicated[54] to find a weak structure

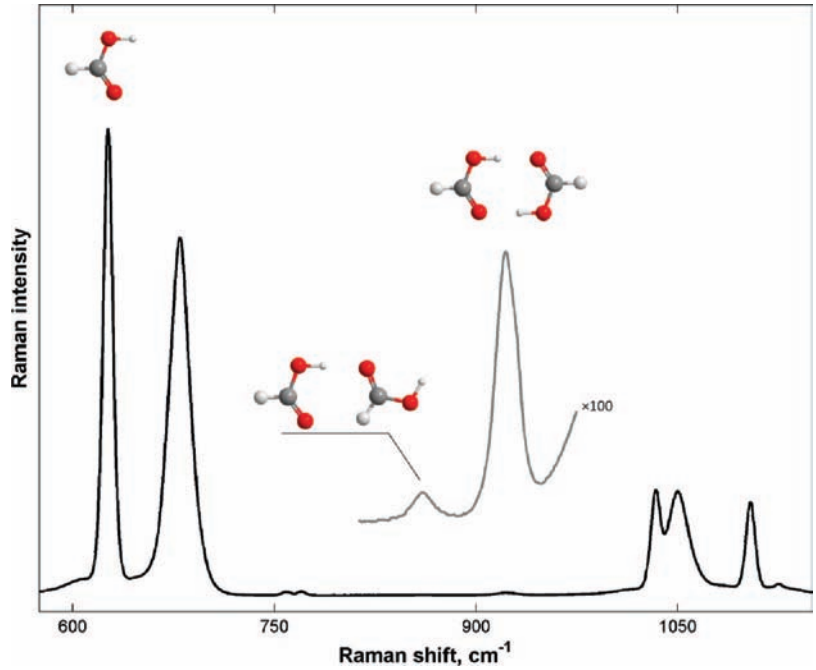

Figure 3. Experimental Raman spectrum of formic acid (575−1150 cm^{-1}) in the gas phase at 25 °C and 4.5 kPa (S/V = 0.25 cm^{-1}). The spectrum is presented after normalization (to the mean value) and Savitzky−Golay filtering (second-order polynomial, a frame size of 11 pixels). The spectrum in the region of 813−975 cm^{-1} with a magnified intensity (×100) is also presented. The band assignment: (FAM) 626.2, 1033.5, and 1104.2 cm^{-1}; (c-FAD, **I**) 679.8, 922, and 1050 cm^{-1}; (a-FAD, **II**) 864 cm^{-1}.

II vibration. Thus, even though FAD **II** Raman activity at 864 cm^{-1} is one of the lowest values, this study makes use of it. Together with a low concentration of O−H···O═C/C−H···O═C (**II**) isomer (∼0.1% at 25 °C), it makes the observation of this peak extremely difficult.

The 864 cm^{-1} peak appearance proves the existence of an isomer of formic acid dimer (**II**) even in the gas phase at conditions close to normal (25−45 °C; 4.5 kPa). Since temperature decrease and pressure increase lead to an increase in dimer fraction (all possible dimers), one would expect the presence of **II** at 20 °C and 1 bar. It should be noted that we are talking about 0.1−1% values.

Note that at the temperatures below 20−25 °C the signal of a-FAD/c-FAD becomes extremely dependent on adsorption.

The standard and simple technique of spontaneous Raman spectroscopy has succeeded in polar FAD identification, while the femtosecond degenerating four-wave mixing (fs DFWM) technique [at room temperature and under supersonic jet conditions (≈60 K)] has not.[30]

3.3.2. Pressure Influence: Do We Observe a Dimer? Even though the results of the previous section look promising, we cannot be convinced that a signal at 864 cm^{-1} belongs to acyclic formic acid dimer (**II**). We cannot check all other possible structures (trimers, tetrames, other oligomers, and inpurities) that can have a Raman-active vibration in the same range, but we can make a simple test to verify that we are dealing with FA dimer. If a vibration at 864 cm^{-1} belongs to dimer (of any structure), the change in pressure should not lead to a change in the intensities ratio of this peak and any other that belongs to other dimers.

Because we are sure that a peak at 679.8 cm^{-1} is a ν_7 (O−C═O) vibration of cyclic FAD, we can use it as a "reference". The intensity ratio of 679.8 and 864 cm^{-1} peaks has been monitored at 25 °C and different total vapor pressures (3.0, 4.5, 6.0, 7.5, and 9.0 kPa). The ratio was found to be constant with respect to the uncertainty interval (approx. 1%). Higher vapor pressure leads to significant adsorption problems.

Presented results show that we are dealing with a HCOOH dimer structure. A monomer, trimer, or tetramer would have a completely different behavior.

3.3.3. Isotope Substitution. Isotope substitution strategy can be very helpful to distinguish isomer vibrations. In our case, it means to distinguish true FAD **II** isomer vibration from hot (or combination) FAD **I** contribution. Unfortunately, in the case of DCOOD, quantum chemistry predicts (and Raman experiment proves) that all a-FAD bands are overlapped by that of c-FAD or FAM. The only exception is a C−D vibration that is predicted to be at 2526 cm^{-1}, but this region of the DCOOD spectrum is too sophisticated to be analyzed (see Figure 2 in ref 28 for details). The same can be said about HCOOD and DCOOH spectra.

One can conclude that isotope substitutions are not applicable to the identification of acyclic FA isomer. It could be that the situation is different for FAD **III**−**VI**.

Note that the presented temperature behavior (Figure 4) is completely different from what can be expected for hot or combination band of FAM/c-FAD.

3.3.4. Thermodynamics of Polar Formic Acid Dimer (II). Using Raman peak intensity ratios, one can plot a van't Hoff isochore. The plot is presented in Figure 4 where the monomer peak at 1104 cm^{-1} and dimer **II** peak at 864 cm^{-1} are used for evaluation of thermodynamic parameters. The values are already corrected for adsorption (see section 3.2.2).

The plot is highly linear—up to the temperature of 38.7 °C ($10^5/T = 320.6\ K^{-1}$). The deviation in a high-temperature region is connected with our inability to accurately determine the 864 cm^{-1} peak area (which decreases with temperature increase). Acid decomposition should not play any role in this temperature region, as we have already discussed in section 3.2.1. In any case, the linearity of the data set is high enough ($R^2 = 0.9966$; RMSE = 0.017) to approximate the plot with a straight line.

Weighted ($1/\sigma$) linear regression has led to a $\Delta H_{\text{a-FAD}}$ value of -8.6 ± 0.2 kcal mol^{-1} (95% confidence interval). This value should be compared with −8.82 kcal mol^{-1} (Table 5) as

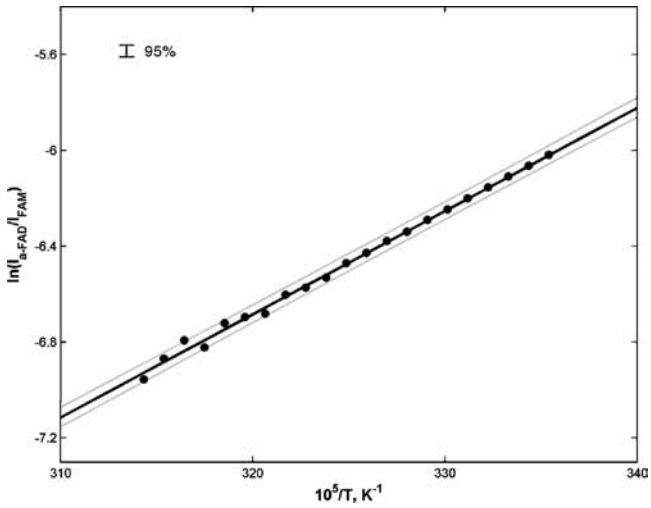

Figure 4. Dependence of the natural logarithm of peak integral intensity ratio [between acyclic dimer (**II**) and monomer of formic acid] on the reverse thermodynamic temperature (black circles). The linear fit ($R^2 = 0.9966$; black line) is presented with 95% error bars (gray lines). The mean 95% confidence interval for the experimental points is presented in the left-upper corner. The interval is approx. 3.5 times larger for high-temperature points than for low-temperature ones. Thermodynamic data (enthalpy and entropy differences): $\Delta H_{\text{a-FAD}} = -8.6 \pm 0.2$ kcal mol^{-1} (-35.8 ± 1.0 kJ mol^{-1}); $\Delta S_{\text{a-FAD}} \approx -36 \pm 2$ cal mol^{-1} K^{-1} (-150 ± 9 J mol^{-1} K^{-1}).

predicted at the MP2/6-311++G(3df,2p) level (BSSE corrected value of ΔE; note that no ZPE or thermal correction has been applied). These values are in good agreement. This fact also proves our assignment of the 864 cm^{-1} vibration (see above).

It seems that the use of the MP2 level of theory with a medium-size basis set leads to an error in energy values of just ~0.5 kcal mol^{-1}. Zero-point energy (ZPE) and thermal corrections (ΔH_T at 298 K) give a value of -7.12 kcal mol^{-1} or 17% less (in absolute values). The difference between experimental and predicted values is more than $7\sigma_{\text{exp}}$. Such a difference could be expected for the MP2/6-311++G(3df,2p) level of theory.

Experimental enthalpy difference can also be compared with a value of -9.1 kcal mol^{-1} (BSSE-corrected ΔE value) obtained by Brinkmann et al.[7] This single-point CCSD(T)/aug′-cc-pVTZ value at the MP2/TZ2P+diff optimized geometry seems to be more reasonable (of course, after ZPE and thermal corrections). So, MP2 agreement seems to be fortuitous.

It should be noted that quantum chemistry data (MP2 and B3LYP) were extremely useful for formic acid gas-phase spectra interpretation and Raman lines deconvolution.

To validate the exactness of our method of enthalpy evaluation, we have conducted the same analysis (van't Hoff isochore) for cyclic FA dimer (**I**). The values of integral intensities of 679.8 (c-FAD) and 1104 (FAM) cm^{-1} peaks were used. The value of -14.9 ± 0.4 kcal mol^{-1} has been obtained. It should be compared with -15.25 kcal mol^{-1} of Chao and Zwolinski (at 298 K).[59] One can see that Raman spectroscopy can provide the exact values of formic acid thermodynamic quantities.

Unfortunately, spectroscopy data (intensities ratio) do not allow fully experimental evaluation of dimerization entropy. Since we cannot experimentally determine the Raman cross section of the FAD **II** peak at 864 cm^{-1}, we need to get these data from other sources. Quantum chemistry data can be such a source.

The MP2/6-311++G(3df,2p) level of theory predicts FAD **II** ν_{14} Raman scattering activity of 0.21 Å^4 amu^{-1} and HCOOH ν_8 activity of 3.0 Å^4 amu.$^{-1}$ Coming from activities to cross sections, one gets a ratio of 0.0882 (-2.43 on a ln scale). This ratio leads to a $\Delta S_{\text{a-FAD}}$ value of -36 ± 2 cal mol^{-1} K^{-1}. The error bars are evaluated with an assumption of ±50% accuracy of predicted activity (cross section) values. The MP2/6-311++G(3df,2p) prediction (in RRHO approximation,[55] using *ab initio* frequencies) for FAD **II** entropy at 4.5 kPa is -37.5 cal mol^{-1} K^{-1}. The values are in good agreement (even though FAD can hardly be called rigid rotor or harmonic oscillator). From Table 5, one can see that all other FAD structures (**III**−**VI**) are on the border or outside the confidence interval.

It should be stated once again that a $\Delta S_{\text{a-FAD}}$ value of -36 ± 2 cal mol^{-1} K^{-1} cannot be regarded as fully experimental, since theoretical values of Raman scattering activities are used.

4. Conclusions

The following conclusions can be drawn:

1. A polar (acyclic) isomer of formic acid dimer (**II**, a-FAD) is observed in a gas phase. Its ν_{14} peak position is found to be at 864 ± 2.1 cm^{-1} using Raman spectroscopy.

2. The presence of acyclic dimer is confirmed by the pressure dependence of Raman band intensity, temperature influence, and a comparison with quantum chemistry data (*ab initio* normal coordinate analysis and thermochemistry).

3. Thermodynamic parameters of polar formic acid dimer (**II**) are experimentally evaluated for the first time. The enthalpy difference ($\Delta H_{\text{a-FAD}}$) is found to be -8.6 ± 0.2 kcal mol^{-1} (95%); the entropy difference value ($\Delta S_{\text{a-FAD}}$) is estimated to be -36 ± 2 cal mol^{-1} K^{-1}.

4. Cyclic dimer (**I**) ν_{11} vibration is observed at 922 ± 1.5 cm^{-1}. Kirklin[53] assignment is confirmed.

The found thermodynamic data could help both theory (molecular dynamics, H-bond research) and experiment (liquid/solid formic acid research, vapor density measurements), since polar dimer fraction (and spectrum) can be estimated. Further research of formic acid in a gas phase (or nonequilibrium conditions) could lead to experimental identification of other dimer structures (**IIc**−**VI**).[56]

Raman spectroscopy has confirmed its effectiveness as a tool for extraction of molecular thermodynamics data.[60] Note that a recent prediction of Yavuz and Trindle[61] that out-of-plane H−O−C vibrations could allow experimental identification of isomers of formic acid dimer (FAD) is fully confirmed. A theoretical prediction that anharmonic correction for this type of vibration can reach 50 cm^{-1} seems to be reasonable.[61]

Acknowledgment. The assistance of Saint-Petersburg State University of Information Technologies, Mechanics and Optics (Saint-Petersburg, Russia) and Ministry of Defence of the Russian Federation (laser, CCD camera, and gas-phase cell) is acknowledged. A. Borisov is acknowledged for technical assistance; I. Samoilenko is acknowledged for computational assistance (soft- and hardware). The author is grateful to the Government of Russian Federation for a special (nominative) scholarship and to the ITERA International Group of companies for a scholarship. Manuscript reviewers are acknowledged for a severe error correction.

References and Notes

(1) Ito, F.; Nakanaga, T. *Chem. Phys. Lett.* **2000**, *318*, 571.
(2) Dreyer, J. *J. Chem. Phys.* **2005**, *122*, 184306.
(3) Leach, S.; Schwell, M.; Talbi, D.; Berthier, G.; Hottmann, K.; Jochims, H.-W.; Baumgärtel, H. *Chem. Phys.* **2003**, *286*, 15.
(4) Smedarchina, Z.; Fernández-Ramos, A.; Siebrand, W. *J. Chem. Phys.* **2005**, *122*, 134309.
(5) Madeja, F.; Havenith, M. *J. Chem. Phys.* **2002**, *117*, 7162.

(6) Karpfen, A.; Thakkar, A. J. *J. Chem. Phys.* **2006**, *124*, 224313.
(7) Brinkmann, N. R.; Tschumper, G. S.; Yan, G.; Schaefer, H. F. *J. Phys. Chem. A* **2003**, *107*, 10208.
(8) Hocking, W. H. *Z. Naturforsch.* **1976**, *31a*, 1113.
(9) Hocking, W. H.; Winnewisser, G. *Z. Naturforsch.* **1976**, *31a*, 995.
(10) Balabin, R. M. *Chem. Phys.* **2008**, *352*, 267.
(11) Millikan, R. C.; Pitzer, K. S. *J. Am. Chem. Soc.* **1958**, *80*, 3515.
(12) Coolidge, A. S. *J. Am. Chem. Soc.* **1928**, *50*, 2166.
(13) Zielke, P.; Suhm, M. A. *Phys. Chem. Chem. Phys.* **2007**, *9*, 4528.
(14) Pauling, L.; Brockway, L. O. *Proc. Natl. Acad. Sci. U.S.A.* **1934**, *20*, 336.
(15) Almenningen, A.; Bastiansen, O.; Motzfeldt, T. *Acta Chem. Scand.* **1969**, *23*, 2848.
(16) Böttcher, C. J. F. Theory of Electric Polarization. In *Dielectrics in Static Fields*; Elsevier: Amsterdam, 1973; Vol. I.
(17) Hertz, H. G. *Prog. Colloid Polym. Sci.* **1978**, *65*, 92.
(18) Johnson, J. F.; Cole, R. H. *J. Am. Chem. Soc.* **1951**, *73*, 4536.
(19) Lazaar, K. I.; Bauer, S. H. *J. Am. Chem. Soc.* **1985**, *107*, 3769.
(20) Hippler, M. *Phys. Chem. Chem. Phys.* **2002**, *4*, 1457.
(21) Voronin, A. U.; Gerasimov, I. V.; Denisov, G. S.; Rutkovski, K. S.; Tokhadze, K. G. *Chem. Phys. Lett.* **1983**, *101*, 197.
(22) Madeja, F.; Havenith, M.; Nauta, K.; Miller, R. E.; Chocholoušová, J.; Hobza, P. *J. Chem. Phys.* **2004**, *120*, 10554.
(23) Chocholoušová, J.; Vacek, J.; Hobza, P. *Phys. Chem. Chem. Phys.* **2002**, *4*, 2119.
(24) Gantenberg, M.; Halupka, M.; Sander, W. *Chem.—Eur. J.* **2000**, *6*, 1865.
(25) Hill, R. A.; Mulac, A. J.; Hackett, C. E. *Appl. Opt.* **1977**, *16*, 2044.
(26) Riddick, J. A.; Bunger, W. B.; Sakano, T. K. *Organic Solvents, Physical Properties and Methods of Purification*; Wiley-Interscience: New York, 1986.
(27) Császár, A. G.; Allen, W. D.; Schaefer, H. F. *J. Chem. Phys.* **1998**, *108*, 9751.
(28) Bertie, J. E.; Michaelian, K. H. *J. Chem. Phys.* **1982**, *76*, 886.
(29) Roszak, S.; Gee, R. H.; Balasubramanian, K.; Fried, L. E. *J. Chem. Phys.* **2005**, *123*, 144702.
(30) Matylitsky, V. V.; Riehn, C.; Gelin, M. F.; Brutschy, B. *J. Chem. Phys.* **2003**, *119*, 10553.
(31) Granovsky, A. A. PC GAMESS version 7.1. http://classic-.chem.msu.su/gran/gamess/index.html.
(32) Møller, C.; Plesset, M. S. *Phys. Rev.* **1934**, *46*, 618.
(33) Head-Gordon, M.; Pople, J. A.; Frisch, J. M. *Chem. Phys. Lett.* **1988**, *153*, 503.
(34) Hertwig, R. H.; Koch, W. *Chem. Phys. Lett.* **1997**, *268*, 345.
(35) Balabin, R. M.; Safieva, R. Z.; Lomakina, E. I. *Chemom. Intell. Lab. Syst.* **2007**, *88*, 183.
(36) Balabin, R. M.; Syunyaev, R. Z. *J. Colloid Interface Sci.* **2008**, *318*, 167.
(37) Balabin, R. M.; Safieva, R. Z.; Lomakina, E. I. *Chemom. Intell. Lab. Syst.* **2008**, *93*, 58.
(38) Maronna, R. A.; Martin, D. R.; Yohai, V. J. *Robust Statistics: Theory and Methods*; Wiley: New York, 2006.
(39) Balabin, R. M.; Safieva, R. Z. *J. Near Infrared Spectrosc.* **2007**, *15*, 343.
(40) Balabin, R. M.; Safieva, R. Z. *Fuel* **2008**, *87*, 1096.
(41) Balabin, R. M.; Syunyaev, R. Z.; Karpov, S. A. *Energy Fuels* **2007**, *21*, 2460.
(42) Balabin, R. M.; Safieva, R. Z. *Fuel* **2008**, *87*, 2745.
(43) Western, C. M. PGOPHER, a Program for Simulating Rotational Structure, University of Bristol. http://pgopher.chm.bris.ac.uk.
(44) Herrebout, W. A.; van der Veken, B. J.; Wang, A.; Durig, J. R. *J. Phys. Chem.* **1995**, *99*, 578.
(45) Pistorius, A. M. A.; DeGrip, W. J. *Vib. Spectrosc.* **2004**, *36*, 89.
(46) Weber, A. *Raman Spectroscopy of Gases and Liquids*; Springer-Verlag: Berlin, 1979; Vol. 11.
(47) Herzberg, G. *Molecular Spectra and Molecular Structure: Infrared and Raman of Polyatomic Molecules*; Krieger Publishing Company: Malabar, FL, 1991.
(48) Hill, W.; Rogalla, D. *Anal. Chem.* **1992**, *64*, 2575.
(49) The difference between **III** and **IV** values seems to be a misprint.
(50) Gibson, H. W. *Chem. Rev.* **1969**, *69*, 673.
(51) Mathews, D. M.; Sheets, R. W. *J. Chem. Soc. A* **1969**, 2203.
(52) Auwera, J. V.; Didriche, K.; Perrin, A.; Keller, F. *J. Chem. Phys.* **2007**, *126*, 124311.
(53) Kirklin, D. R. Ph.D. Thesis, University of Maryland, 1975.
(54) Bertie, J. E.; Michaelian, K. H.; Eysel, H. H.; Hager, D. *J. Chem. Phys.* **1986**, *85*, 4779.
(55) Jensen, F. *Introduction to Computational Chemistry*; John Wiley & Sons: New York, 1998.
(56) Marushkevich, K.; Khriachtchev, L.; Lundell, J.; Rasanen, M. *J. Am. Chem. Soc.* **2006**, *128*, 12060.
(57) Florio, G. M.; Zwier, T. S.; Myshakin, E. M.; Jordan, K. D.; Sibert, E. L. *J. Chem. Phys.* **2003**, *118*, 1735.
(58) Lide, D. R. *CRC Handbook of Chemistry and Physics*, 84th ed.; CRC Press: Boca Raton, FL, 2003.
(59) Chao, J.; Zwolinski, B. J. *J. Phys. Chem. Ref. Data* **1978**, *7*, 363.
(60) Balabin, R. M. *J. Phys. Chem. A* **2009**, *113*, 1012.
(61) Yavuz, I.; Trindle, C. *J. Chem. Theory Comput.* **2008**, *4*, 533.

JP9002643